Implementation of a free boundary condition to Navier-Stokes equations

Morten M.T. Wang and Tony W.H. Sheu
Department of Naval Architecture and Ocean Engineering, National Taiwan University, Taipei, Taiwan, Republic of China

Received July 1995
Revised April 1996

Introduction

Numerical prediction of flow physics involves the specification of boundary conditions to close the problem. Whether all or part of the boundary needs consideration depends on the nature of the investigated partial differential equations. Taking as an example, closure boundary conditions for Navier-Stokes equations at an incompressible limit take different forms because a time-dependent problem is classified as elliptic-parabolic while it is elliptic in its steady counterpart. Even though we are under the restraint of mathematic classification, in an attempt to obtain a weak-form solution we may impose boundary conditions according to the physics since boundary conditions, no doubt, come from nature.

Many flow problems of practical relevance in oceanography and meteorology are defined in a fairly large spatial domain. For some flow problems, like ocean circulation, air pollution, and weather prediction, we need to truncate the physically unbounded domain because of CPU-restrictions, memory-limitations, etc. The ambiguity regarding synthetic boundary conditions poses significant computational difficulties since information is hardly available there. Use of an erroneous outlet boundary condition leads sometimes to numerical instability and very often to appreciable inaccuracy in the interior solution. This has motivated researchers, in the community of computational mechanics, to make efforts towards circumventing this difficulty. We may fabricate outlet boundary by intuition and experience. Inclusion of a far-field perturbation solution or a buffer layer in the analysis is also referred to. In general, these “cures” are problem-dependent and fail to properly represent the local physics in reality. As a consequence, we have felt the need for a treatise on developing a viable outflow boundary condition which can mimic or retain the local real behaviour.

We have organized this paper as follows: in the second section, we present Navier-Stokes equations in the form of primitive working variables which are then discretized by a mixed finite element method. In the third section, we discuss some existing outflow boundary conditions and some important issues regarding the consequences of the imposed outlet boundary conditions. We bring forward here a new outflow boundary condition. In the fourth section, we present the computed results of an analytical problem for the validation

International Journal of Numerical Methods for Heat & Fluid Flow
Vol. 7 No. 1, 1997, pp. 95-111.

purpose, followed by a backward facing step benchmark problem and a problem of practical relevance. In the final section, we offer conclusions.

Theoretical formulation

In the present study, we consider the following time-independent set of partial differential equations for the solutions of an incompressible fluid flow:

$$(\underline{u} \cdot \nabla \underline{u}) = -\nabla p + \frac{1}{Re} \nabla^2 \underline{u} \,, \tag{1}$$

$$\nabla \cdot \underline{u} = 0 \,, \tag{2}$$

where $Re = u_0 L/v$ stands for the Reynolds number, L is the characteristic length, u_0 the characteristic velocity, and v the kinematic viscosity of the fluid.

In considering governing equations which are classified as elliptic, we demand that boundary conditions be prescribed on the entire boundary of the physical domain. In order to close the differential equations (1-2), we specify velocities at Γ_D

$$\underline{u} = \underline{g} \,. \tag{3}$$

Besides the above imposed Dirichlet velocities, the following Neumann type boundary condition is needed at the open boundary Γ_N having the unit outward normal vector n:

$$-p\underline{n} + \frac{1}{Re}\frac{\partial \underline{u}}{\partial n} = \underline{f}_{traction} \,. \tag{4}$$

When simulating an incompressible fluid flow, we demand that divergence-free discrete velocities be attainable. Attempts to ensure that the fluid flow is everywhere and always incompressible have dominated the subject of computational fluid dynamics. We analyse equations (1-4) by using a mixed formulation rather than by using a segregated approach so that the mass and momentum conservations can be simultaneously coupled[1-3]. The pressure in the incompressible Navier-Stokes equations serves as a Lagrangian multiplier[4]. As a result, accurate predicted discrete solenoidal velocities may accompany a non-smooth pressure. Legitimate choice of finite element trial spaces for primitive variables is thus of importance because the mixed finite element method is subject to the LBB (Ladyzhenskaya-Babŭska-Brezzi) stability condition[5-7]. To retain a sufficiently smooth solution for the investigated elliptic system (1-4), we take an element free of the LBB stability constraint into consideration. By substituting the well-paired bilinear interpolation function for the pressure and the biquadratic interpolation function for the velocities into the weighted residual statement of (1-2), we can derive the following matrix equations along with the bilinear test function for the mass conservation equation:

$$\int_{\Omega^h} \begin{Bmatrix} C^{ij} & 0 & -M^j \frac{\partial N^i}{\partial X_1} + B^i \frac{\partial M^j}{\partial X_1} \\ 0 & C^{ij} & -M^j \frac{\partial N^i}{\partial X_2} + B^i \frac{\partial M^j}{\partial X_2} \\ M^i \frac{\partial N^j}{\partial X_1} & M^i \frac{\partial N^j}{\partial X_2} & 0 \end{Bmatrix} \mathrm{d}\Omega^h \begin{Bmatrix} u_j \\ v_j \\ p_j \end{Bmatrix} = \underline{F} \,, \tag{5}$$

where

$$C^{ij} = (N^i + B^i)(N^j \tilde{V}_k^j)\frac{\partial N^j}{\partial X_k} + \frac{1}{Re}\frac{\partial N^i}{\partial X_k}\frac{\partial N^j}{\partial X_k} , \tag{6}$$

$$\underline{F} = -\int_{\Gamma^h_{out}} N^i \begin{Bmatrix} pn_x - \frac{1}{Re}\frac{\partial u^j}{\partial n} \\ pn_y - \frac{1}{Re}\frac{\partial v^j}{\partial n} \\ 0 \end{Bmatrix} d\Gamma^h . \tag{7}$$

It remains to define test functions for placing weights on the momentum equations to resolve non-linear velocity oscillations. While the discretized system is stabilized, introduction of biased weighting functions may contaminate the solution. The deterioration in accuracy is mainly attributable to the false diffusion error which arises from the multi-dimensional flow simulation. To achieve stable and accurate solutions, we present a Petrov-Galerkin finite element model. Furthermore, this upwind model belongs to a variant of the streamline upwind schemes on the condition that the biased weighting functions are chosen as:

$$B^i = \tau(N^j \tilde{V}_k^j)\frac{\partial N^i}{\partial X_k} . \tag{8}$$

As with the Streamline-Upwind Petrov-Galerkin (SUPG) method[8], the parameter τ needs to be determined. In the present two-dimensional study, τ is constructed by carrying out an operator splitting procedure. As a result, the expression for τ takes the following form:

$$\tau = \frac{\delta(\gamma_\xi)\tilde{V}_\xi h_\xi + \delta(\gamma_\eta)\tilde{V}_\eta h_\eta}{2|\tilde{V}|^2} . \tag{9}$$

The coefficient δ will be analytically derived as follows in the sense that nodal exactness is achievable in the single dimension. In a domain comprising quadratic elements, the finite element solutions remain nodally exact if we demand that

$$\gamma_\xi = \tilde{V}_\xi h_\xi Re/2 \; ; \quad \gamma_\eta = \tilde{V}_\eta h_\eta Re/2 ,$$

$$V_\xi = \hat{\mathbf{e}}_\xi \cdot \tilde{V} \; ; \quad V_\eta = \hat{\mathbf{e}}_\eta \cdot \tilde{V} ,$$

$$\delta(\gamma) = \frac{1}{2}\coth(\frac{\gamma}{2}) - \frac{1}{\gamma} ,$$

where $\hat{e}_\xi$ and $\hat{e}_\eta$ are the local co-ordinate basis unit vectors. In the course of finite element calculations, linearization procedure is performed, as exemplified by the linearized velocity

$$\tilde{V}^{(n+1)} = (1-\omega)V^{(n-1)} + \omega V^{(n)} .$$

Here, we denote the superscript (n) as the n-th iteration number while ω is the user's specified relaxation factor.

This section concludes with a brief description of the solution algorithm, by which primitive variables are obtained simultaneously. The analysis begins with a guessed velocity field from which the global stiffness matrix can be formed. The coupled system of algebraic equations being linearized is then solved subjected to the boundary conditions, which are the main theme of the next section, on the truncated outlet. We will terminate the iteration procedures, in so far as all convergent tolerances reach the users specified values. Worthy to note is that the resulting algebraic equations are classified as being unsymmetric and indefinite and are amenable to the conventional frontal direct solver[9].

Boundary condition

General remarks and literature review

To the authors' best knowledge, a permissible boundary condition applicable to through-flow problems has not been found yet. At a solid wall or a free surface, one can apply physical arguments to render boundary conditions. Unlike the closure conditions which are derivable at a solid or a free surface boundary, one often makes the analysis domain smaller than the real domain. As a result, no physical reasoning is available for us to derive physically plausible outflow conditions because downstream behaviour is unknown and is hard to predict. In fact, there will never be an ultimate answer. For computational reasons, the physical domain needs to be truncated at a synthetic boundary where the surface traction vector, f_{traction}, defined in equation (4) is not known a priori. This ambiguity is particularly pronounced when a simulation involves a solid boundary to which a boundary layer is attached. Under this circumstance, it is hoped that the artificial boundary will be far away from the inlet to prevent unphysical feedback noises, emanating from the outflow boundary, from being propagated upstream, and from destroying the solution. Even for problems having very large extension in size, the analysis domain must be truncated somewhere; otherwise, the disk storage and the computer time will be prohibitive. This implies that there exists a dilemma in determining the trade off between these two considerations.

Over the past few decades, considerable research has been devoted to studying the consequences of applying artificial outflow conditions to truncated boundary. Much of the previous works in this area have focused on compressible flow. For an inviscid Euler fluid flow, analytical open boundary conditions which pertain to the truncated boundary are derivable from differential equations of the hyperbolic type. However, artificial conditions underlying the Sommerfeld radiation condition or method of characteristics hold only for a limited flow realm. It goes without saying that these conditions can be applied to incompressible Navier-Stokes flow simulations. Nevertheless, the Sommerfeld boundary condition remains as one of the most popular open boundary conditions.

As to the open boundary conditions applicable to an incompressible Navier-Stokes fluid flow, there have been comparatively few developments. In the open

literature, there exist several techniques which have been reported to be effective in circumventing computational difficulties in association with the large extent of the fluid domain. We broadly classify them into four major classes:

(1) imposition of a boundary condition by physical intuition;

(2) a hybrid coupling of the discretization method with an infinite element[10] or a boundary element[11];

(3) non-reflecting boundary condition[12]; and

(4) free boundary condition[13].

Within the realm of the first class of outflow boundary conditions, there exist several variants. These underlying concepts differ in the implementation of physical intuition so as to yield a boundary condition of the Dirichlet or Neumann type. While these methods have an overwhelming advantage in numerical implementation, they lack the underlying analytic evidence. Simplified equations of motion have been applied at the outlet boundary to study gradually developing flow[14]. More analytically, Chen and Jiang[15] have specified velocities at the outflow boundary as the sum of those at the far-field and its analytically derivable perturbed velocities based on the corresponding steady incompressible Navier-Stokes equations.

Nonreflecting boundary conditions are devised to absorb waves incident on the boundary. This class of outflow boundary conditions abounds in the literature. For a good review of nonreflecting boundary conditions, the reader is referred to Jin and Braza[12], who have made remarks on the works of Engquist and Majda[16,17], Rudy and Strikwerda[18], Hedstrom[19], Thompson[20], Halpern[21], Bayliss and Turkel[22], and Nataf[23]. Liu and Lin[24] followed a different line to resolve erroneous noise by attaching a buffer layer to the physical domain. The reflected outgoing waves from an artificially truncated outlet are thus absorbed. In each momentum equation, they added a buffer function only to the streamwise second-order derivatives. This aids damping of the erroneous fluctuations.

Until recently, techniques like perturbation and asymptotic analyses have been applied to flow equations between a synthetic boundary and far downstream where matters are not disturbed. These approaches, however, are feasible only when the flow downstream from the synthetic outflow is amenable to asymptotic analysis. In regions sufficiently far from the object, in the case of an external flow simulation, or far from the inlet in the case of an internal flow analysis, the Navier-Stokes equations can be rationally linearized about the constant state at infinity. Johansson[25], and Halpern and Schatzman[26] adopted this idea to design their outflow boundary condition by linearizing the incompressible, time-dependent Navier-Stokes equations about a constant flow and then solving the reduced equations of a much simpler form analytically in the Fourier space using a Laplace-Fourier technique. In this context, Johansson[25] suggested a set of outlet boundary conditions. These boundary conditions, although quite mathematically involved, cannot be regarded as

exact outflow boundary conditions since an assumption on the linearization of advective fluxes has been made.

Free boundary condition

Prior to solving the unsymmetric and indefinite matrix equations, normal and tangential components of the surface traction vector f_{traction} at the synthetic outlet are needed. The difficulty is that the exact stresses are unknown a priori at the synthetic outlet; thus, any erroneous boundary stress will result in unphysical reflection waves and cause a significant distortion of solutions in the interior. This, together with the fact that approaches, as was discussed in Section 3.1, hold only for a limited flow condition and certain type of equation, makes the search for another means of alleviating fundamental difficulty becomes indispensable.

In this paper, we extend the validity of the mixed finite element formation to the outlet without imposing an ad hoc stress boundary condition at the artificial boundary. This corresponds to regarding the surface traction vector f_{traction} as unknown, serving as a part of solutions to be computed. The flow structure upstream of the outlet boundary remains unaltered in the circumstances. This is equivalent to computing primitive variables ($\underline{u}$, p) directly from the matrix equations:

$$\underline{\underline{A}} \begin{Bmatrix} u_j \\ v_j \\ p_j \end{Bmatrix} - \underline{F} = \underline{0} \ .$$

It is noteworthy that the underlying boundary condition matches the outflow physics exactly with the Navier-Stokes equations which are well defined inside the domain. As a consequence, both non-linear and diffusive fluxes in the flow can be taken into account.

Test problem and results

Analytic validation

Prior to simulating a realistic flow problem, it is important to verify the applicability of the proposed finite element model to the simulation of a problem involving an attached boundary condition. A test problem amenable to analytic solutions is, thus, desirable. In a square domain of length 1, the problem investigated is subject to the boundary conditions defined in Figure 1. According to the analytic solutions given by

$$u = y(1 - y) \ ,$$

$$v = 0 \ ,$$

$$p = \frac{2}{Re}(1 - x) \ ,$$

the boundary condition at the outlet corresponds to a traction-free outflow boundary condition. In this calculation, analyses are carried out in a square which is uniformly discretized with different resolutions, namely 5×5, 10×10, 20×20, 40×40. With the computed global $L_{2\_}$ error norms, we can estimate the rates of convergence for both working variables from Table I. As Figure 2 indicates, *y*-independent pressure distribution is obtained which takes the same

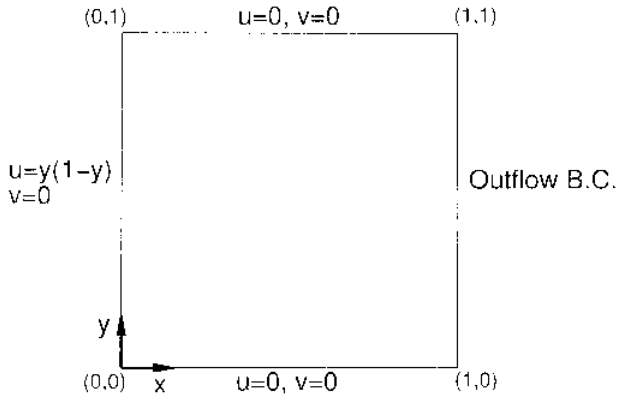

Figure 1.
Illustration of the analytic problem given in this section

Mesh size	$\|\|\underline{u}-\underline{u}_{exact}\|\|$	Convergent order	$\|\|p-p_{exact}\|\|$	Convergent order
mesh 5×5	$1.193 \times 10{-}4$		$5.504 \times 10{-}5$	
mesh 10×10	$5.364 \times 10{-}5$	1.153	$2.147 \times 10{-}5$	1.358
mesh 20×20	$2.130 \times 10{-}5$	1.332	$7.451 \times 10{-}6$	1.527
mesh 40×40	$6.870 \times 10{-}6$	1.632	$2.252 \times 10{-}6$	1.726

Table I.
Error of L_2 norm and convergent order for the analytic problem defined in Section 4.1

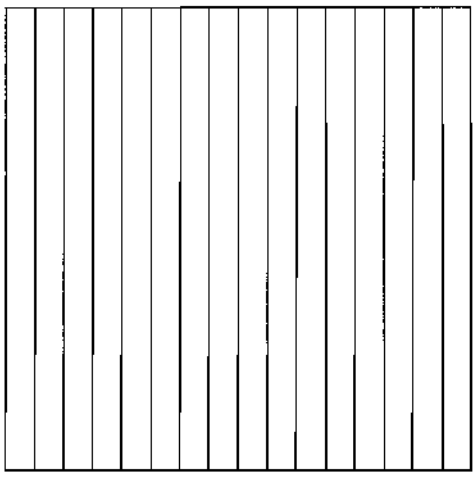

Figure 2.
Computed pressure contours for the analytic problem given in this section

form as the analytic pressure given in (10). For completeness, we also plot the reduction of residuals against the iteration in Figure 3 for each primitive variable. Fairly good convergence behaviour is demonstrated.

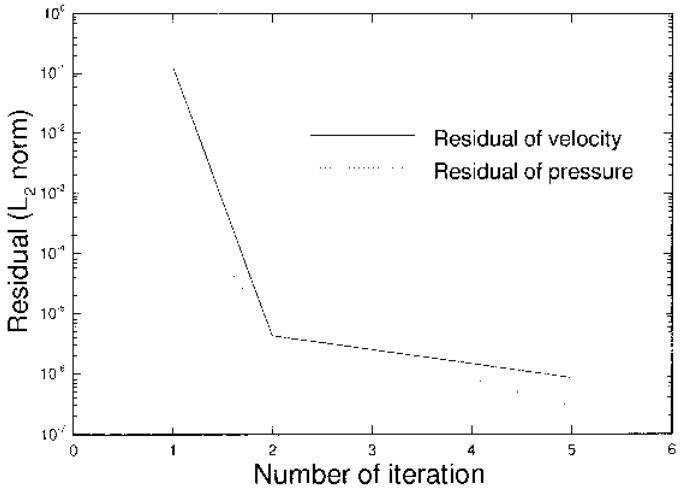

Figure 3.
Convergent history for the analytic problem

Backward-facing step internal flow problem

The flow over a backward-facing step is best-suited to confirming the effectiveness of the free boundary condition applied at the synthetic boundary. The widespread popularity of this problem is attributable to the well-documented experimental and numerical data. In fact, this problem was chosen as a benchmark test by the Minisymposium on Open Boundary Conditions held at Stanford University on 14 July 1991. While the flow under consideration has a regular configuration, the flow physics illustrated in the interior passage are far from simple since in the course of flow development it undergoes a series of detachment-and-reattachment processes. Referring to Figure 4 which depicts the investigated configuration, the aspect ratio of the height of backward-facing step s to the width of the cross-sectional H is s: H = 1 : 2.

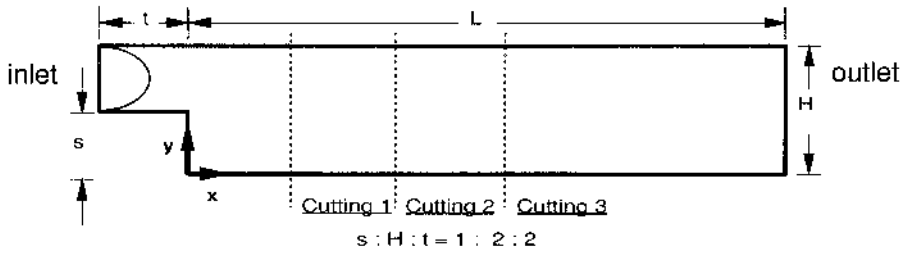

Figure 4.
Illustration of the backward-facing step problem defined in this section

At the inlet which is upstream of the step with a length of H, we have specified a parabolic velocity profile. This corresponds to saying that the flow has been fully developed. No-slip conditions were imposed at solid walls. In the present study, we consider a Reynolds number which still exhibits a steady and visible secondary eddy at the top wall. According to the characteristic velocity $\bar{u} = 2/3U_{max}$ and the characteristic length H, the Reynolds number is 800.

With the finite element grids illustrated in Figure 5 we can analyse the flow upstream of the step, and thereby account for the geometric singularity at the step corner. In this paper, we are interested in studying the influence of the truncated length on the circulation eddy established just behind the step, followed by a downstream upper secondary eddy. With a fine mesh in the smaller channel of length $2s$ just upstream of the step, the physical domain of largest size contains 1,440 non-uniform biquadratic elements. Hereafter, the shorter domain refers to the length of L is shorter than L_{max}.

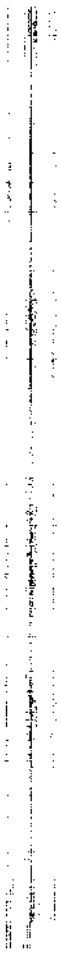

Figure 5.
Finite element mesh of the backstep problem

To begin with, we have carried out the calculation on the basis of $L = 66s$, as measured from the step. According to the computed results in Figure 6, the velocity profile in close proximity to the exit has reached full development (Hagen-Poiseuille). We take these solutions as being exact. Several shorter cases with cutting planes at $L/s = 10$, $L/s = 20$, and $L/s = 32$ are also investigated. Test problems with different lengths of L are carried out, of course, using the same computer code. Figure 7 explains why reliable analysis needs to be analysed at a truncated length, at least at $L/s = 32$. For L/s beyond 32, the traction forces approach fairly close to zero.

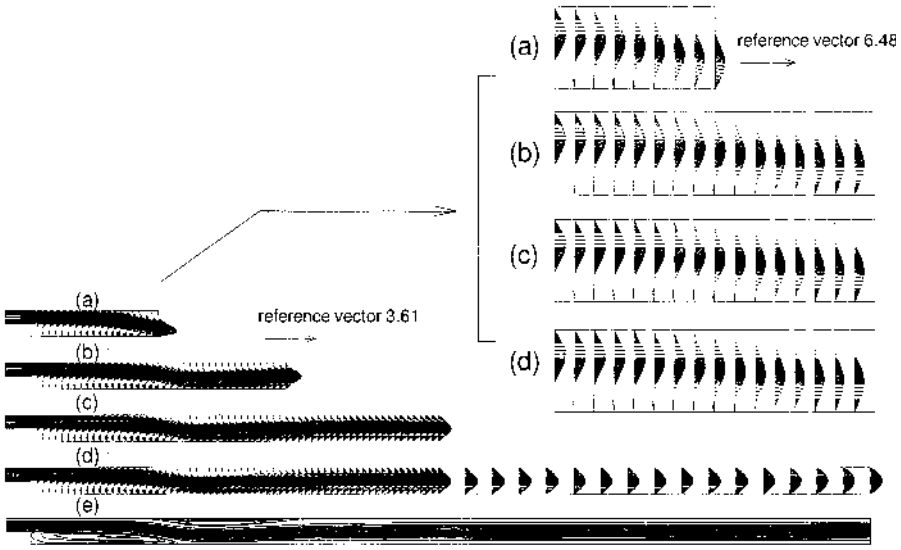

Figure 6.
Velocity vectors and streamlines inside the flow domains of different truncated lengths, (a) $L/s = 10$; (b) $L/s = 20$; (c) $L/s = 32$; (d) $L/s = 66$; (e) $L/s = 66$

We denote x_1 as the computed reattachment length of the recirculating zone behind the step. We also define x_2 as the location of detachment and x_3 as the location of reattachment of secondary recirculating zone near the upper wall. These values are plotted in Figure 8 for $L/s = 10$, 20, 32, 66, respectively, and compare with the FIDAP results of Sohn[27], finite difference results of Durst and Pereira[28], and experimental data of Armaly *et al.*[29]. The reattachment length obtained does not match well with the experimental results, probably owing to the fact that the experimental work of Armaly *et al.* was carried out at $H/s = 2.061$ while 2 in the numerical simulation. For cases other than $L/s = 66$, the disagreement might be attributed to the fact that the channel length (L) is too short to permit flow development. Of note is that when the Reynolds number is greater than 400, the computed reattachment length differs from the experimental measurement in that the flow becomes three-dimensional.

As seen from the residual reduction plot in Figures 9 and 10, convergent solutions for each truncated boundary are attainable. The smaller the physical domain is, the faster the convergent rate is. Also of note is that some shorter

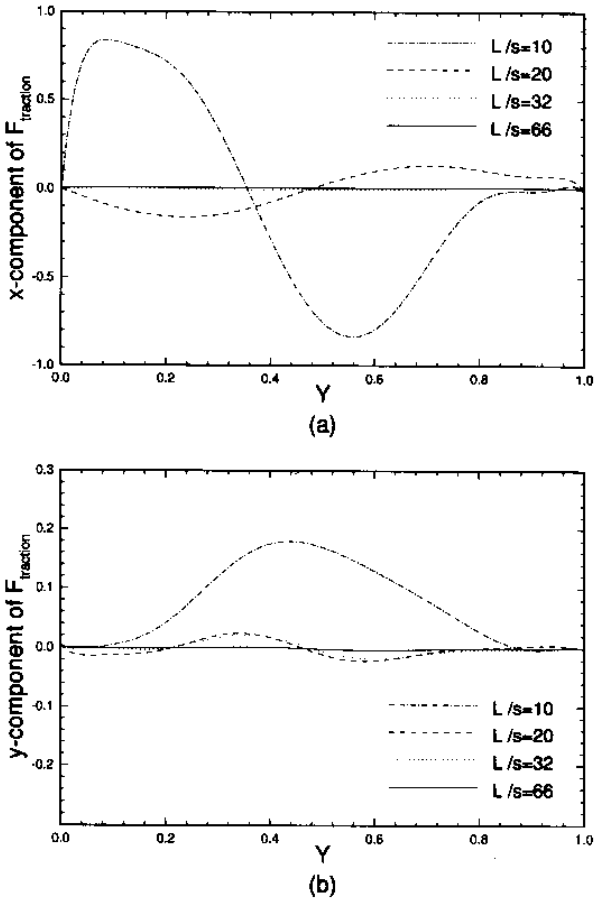

Figure 7. Computed traction forces at the investigated truncated lengths: (a) *x*-component of the traction force vector defined in equation (4); (b) *y*-component of the traction force vector defined in the equation (4)

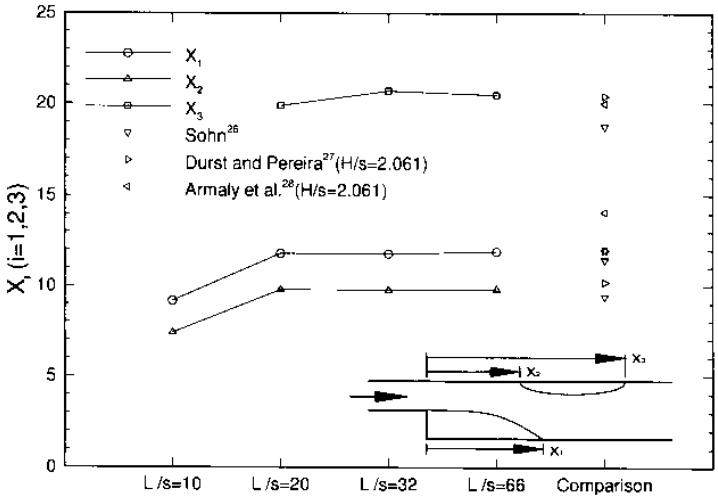

Figure 8. Predicted locations of the flow detachment and reattachment and the referred comparison locations

truncated outlets cut across the developing recirculation eddies. Indicated by these figures is that a guessed channel length may mask the physical reality. Consequently, a problem accommodating the free boundary condition is worth investigating. Also of importance is that the presence of the reversed flow at the synthetic boundary can be well-predicted. Through numerical experimentation, we have found that the grid needs to be finely graded, otherwise the solution might diverge.

By examining the convergent solutions shown in Figure 6 for problems having different truncated lengths, we have found that the solution accuracy deteriorates for the case having a shorter domain because insufficient downstream information has been conveyed through the wall-attached

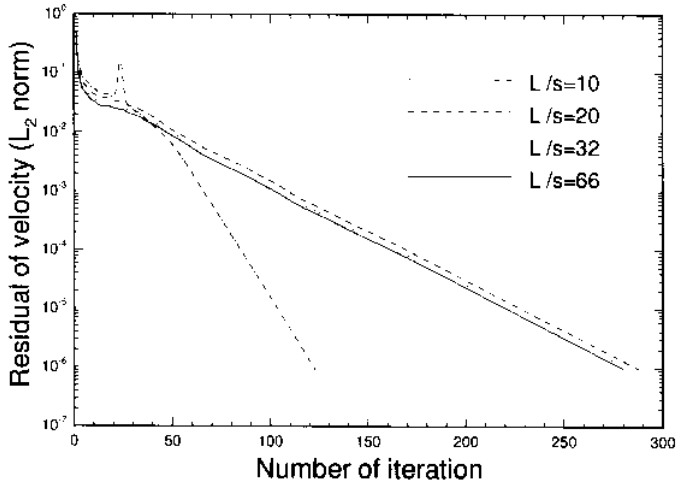

Figure 9.
Velocity convergent history for backward-facing step problem on four different truncated lengths

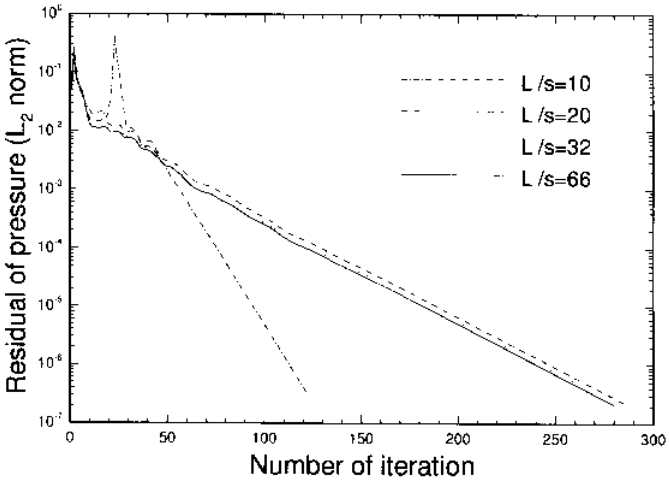

Figure 10.
Pressure convergent history for backward-facing step problem on four different truncated length

boundary layers. Figure 11 plots the outlet normal velocity profile on different truncated lengths. As is clearly illustrated in Figure 11 and Table II global mass conservation is obtained from the present mixed formulation.

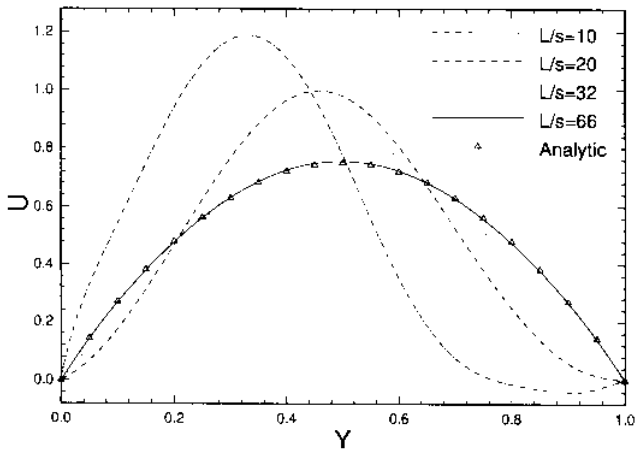

Figure 11. Outlet velocity distribution for the backward-facing step problem having four different truncated lengths. (Δ: fully developed velocity profile)

Table II. Mass ratio of outlet flow to inlet flow and L^2 norm of the deviation between outlet normal velocity and fully developed velocity

	L/s = 10	L/s = 20	L/s = 32	L/s = 66
Q_{outlet}/Q_{inlet}	0.99608	0.99969	0.99973	0.99970
$\|\|U_c - U_{fd.}\|\|$	0.39002	01.6004	0.05230	0.00325

Flow analysis in a wharf

With an increasing demand for electric power supply, discharged thermal pollution from power stations in coastal areas has drawn considerable attention. For cooling purposes, sea water is inducted. After undergoing a circulation cycle, the heated water is finally discharged back into the ocean environment. The resulting temperature increase due to these discharges might affect living species or cause inconvenience and permanent damage to the environment. Resolution of the conflict between environmental protection and economic growth thus depends heavily on the design quality of the discharging system. Under incompressible circumstances, the flow and thermal fields are decoupled. Information about the discharged flow structure is, thus, of importance to satisfy the environmental emission regulation.

The present study has attempted to provide the velocity distribution around the Sen Au fish wharf, near the north part of Taiwan, where a fuel-fired thermal power plant is located. The coastal line of the Sen Au wharf is depicted in

Figure 12, where $\overline{al}$ represents the drainage outlet. A mode, as represented by $\overline{ijkl}$ and $\overline{bcde}$ was constructed for the prevention of severe sea waves and currents. To provide readers with an idea of the size of the problem under investigation, we choose a characteristic length $\overline{al}$ for reference which takes a length of 187m. Admittedly, to simulate such a large-scale flow problem in a three-dimensional context, it is computationally infeasible within the framework of mixed finite element model. To make the problem amenable to computers presently available, we need to reduce the problem to two dimensions and truncate the outflow boundary to $\overline{O_1O_2O_3O_4}$ for the sake of disk storage restriction. By applying the technique of the free boundary condition, we can effectively obtain the velocity vector plots, shown in Figure 13. With these velocities, the temperature distribution can be rendered by solving the energy equation, which takes the form of a scalar convection-diffusion equation.

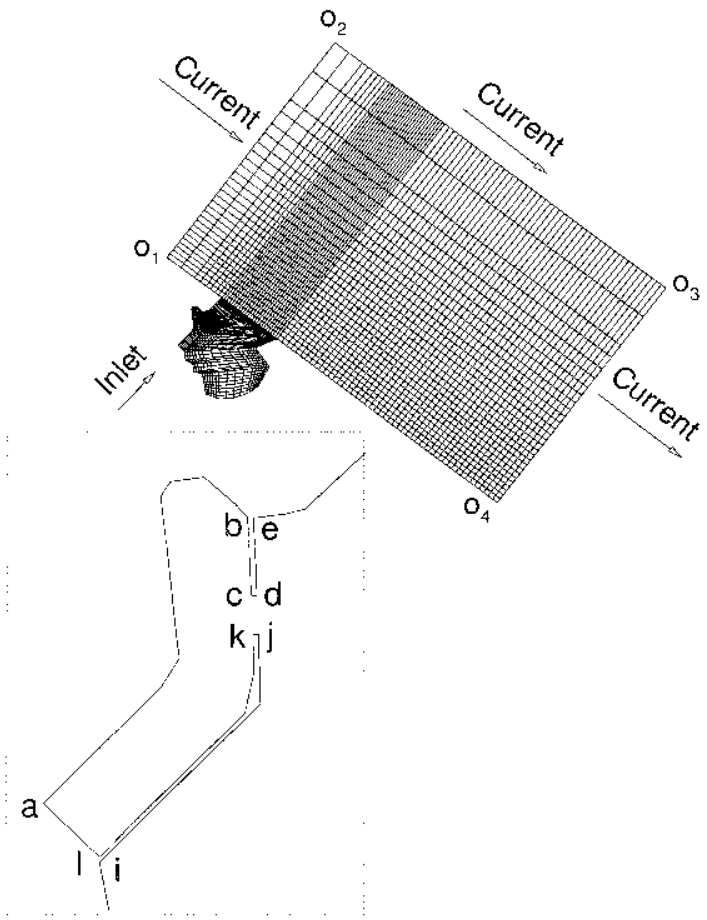

Figure 12.
Illustration and mesh for the flow analysis in a wharf

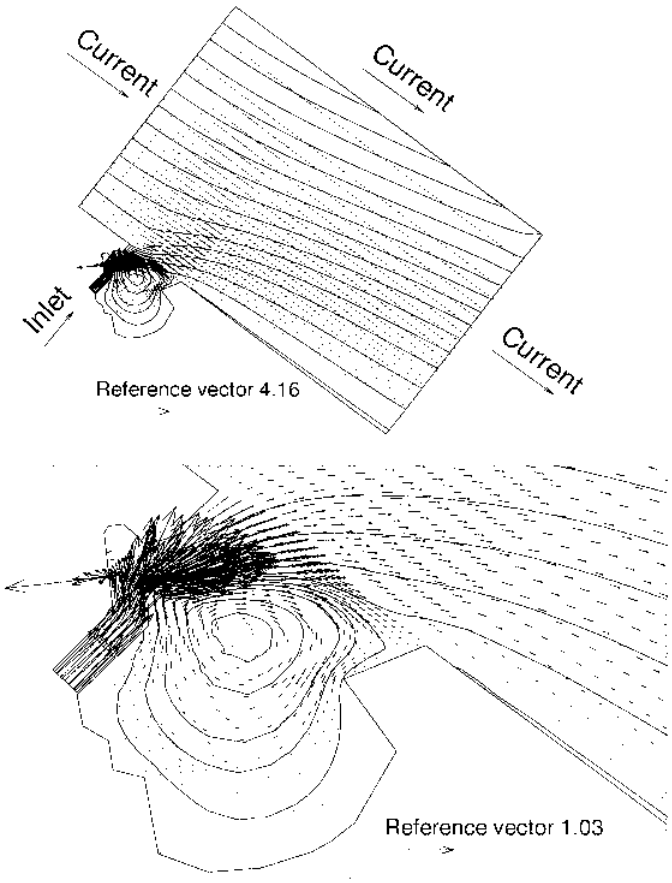

Figure 13.
Velocity vectors and streamlines for flow analysis in a wharf

Conclusions

As truncated boundaries do not exist in reality, there is no genuine physical reasoning for deriving open boundary conditions. Nevertheless, we have to make the calculation domain smaller than the physical domain by specifying appropriate boundary conditions there.

For constructing open boundary conditions, we need not impose any constraint condition at the synthetic outlet, but rather extend the validity of the weighted residual finite element equations to the truncated boundary to prevent the interior solution profile from being distorted by the feedback noises. This approach indeed yields a convergent solution regardless of where the open boundary is truncated and whether the reversed flow appears at the artificial open boundary or not. The difference is only evidenced by a slight deterioration of convergence rate when the synthetic open boundary intersects the circulation bubble. With the convergent solutions, the developing stresses at the truncated outlet can be computed a posteriori. If these stresses approach the user specified

zero, the computed convergent solutions within the whole domain can also be regarded as accurate. If not, the solutions have room for further improvement. This can be simply achieved by enlarging the computational domain while keeping the original grid system unchanged. In other words, we pursue numerical solutions in the truncated domain which are close to those found in the infinite domain. The extension length from the open boundary is determined a priori from the previously computed line integral containing the traction vector. It is worth emphasizing that in the present method there is neither artificial specification of an open boundary condition nor tedious mathematic derivation. The proposed outflow boundary treatment is clean and robust. Based on the test problems considered and the results obtained, we can confirm the validity of the proposed boundary treatment.

References

1. Gunzburger, M.D., *Finite Element Methods for Viscous Incompressible Flows: A Guide to Theory, Practice and Algorithms*, Academic Press, New York, NY, 1989.
2. Girault, V. and Raviart, P.A., *Finite Element Methods for Navier-Stokes Equations,* Springer-Verlag, Berlin, 1986.
3. Temam, R., *Navier-Stokes Equations, Theory and Numerical Analysis*, North-Holland, Amsterdam, rev. ed., 1979.
4. Ladyzhenskaya, O., *The Mathematical Theory of Viscous Incompressible Flow*, Gordon and Breach, New York, NY, 1969.
5. Brezzi, F. and Douglas, J., "Stabilized mixed methods for the Stokes problem", *Numer. Math. 53*, 1988, pp. 225-35.
6. Babuska, I., "The finite element method with Lagrange multipliers", *Numer. Math.,* Vol. 20, 1973, pp. 179-92.
7. Brezzi, F., "On the existence, uniqueness and approximation of saddle point problems arising from Lagrangian multipliers", *RAIRO, Anal. Num.,* Vol. 8 (R2), 1974, pp. 129-51.
8. Hughes, T.J.R., Franca, L.P. and Becestra, M., "A new finite element formulation for computational fluid dynamics, V. circumventing the Babuska-Brezzi condition, A stable Petrov-Galerkin formulation of the Stokes problem accommodating equal-order interpolations", *Comput. Methods Appl. Mech. Eng.*, Vol. 59, 1986, pp. 85-99.
9. Irons, B.M., "A frontal solution for finite element analysis", *Int. J. Numer. Meth. Eng.,* Vol. 2, 1970, pp. 5-32.
10. Saini, S.S., Bettess, P. and Zienkiewicz, O.C., "Coupled hydrodynamic response of concrete gravity dams using finite and infinite elements", *Earthquake Engrg. Struct. Dyn.*, Vol. 6, 1978, pp. 363-74.
11. Felippa, C.A., "Interfacing finite element and boundary element discretizations", *Appl. Math. Modell.*, Vol. 5, 1981, pp. 383-6.
12. Jin, G. and Braza, M., "A non-reflecting outlet boundary condition for incompressible unsteady Navier-Stokes calculations", *J. Comp. Phys.,* Vol. 107, 1993, pp. 239-53.
13. Papanastasiou, T.C., Malamataris, N. and Ellwood, K., "A new outflow boundary condition", *Int. J. Numer. Methods Fluids,* Vol. 14, 1992, pp. 587-608.
14. Miyauchi, T., Tanahashi, M. and Suzuki, M., "Boundary conditions for direct numerical simulations of spatially developing flows", in *Proceedings of the 5th Int. Symp. on Computational Fluid Dynamics,* Vol. 2, Sendai, 1993, pp. 261-6.
15. Yaosong, C. and Tao, J., "An open boundary condition for N. S. equations", in *Proceedings of the 5th Int. Symp. on Computational Fluid Dynamics,* Vol. 1, Sendai, 1993, pp. 101-07.

16. Engquist, B. and Majda, A., "Absorbing boundary conditions for the numerical simulation of waves", *Math. Comput.,* Vol. 31, 1977, pp. 629-51.
17. Engquist, B. and Majda, A., "Numerical radiation boundary conditions for unsteady transonic flow", *J. Comp. Phys.*, Vol. 40, 1981, pp. 91-103.
18. Rudy, D.H. and Strikwerda, J.C., "Boundary conditions for subsonic compressible Navier-Stokes calculations", *Comput. Fluids*, Vol. 9, 1981, pp. 327-38.
19. Hedstrom, G.W., "Nonreflection boundary conditions for nonlinear hyperbolic systems", *J. Comp. Phys.*, Vol. 30, 1979, pp. 222-37.
20. Thompson, K.W., "Time dependent boundary conditions for hyperbolic systems", *J. Comp. Phys.,* Vol. 68, 1987, pp. 1-24 .
21. Halpern, L., "Artificial boundary conditions for the linear advection-diffusion equation", *Math. Comput.*, Vol. 46, 1986, pp. 425-38.
22. Bayliss, A. and Turkel, E.,"Far field boundary conditions for compressible flows", *J. Comp. Phys.,* Vol. 48, 1982, pp. 182-99.
23. Nataf, F., "An open boundary condition for the computation of the steady incompressible Navier-Stokes equations", *J. Comp. Phys.*, Vol. 85, 1989, pp. 104-29.
24. Liu, C and Lin, Z., "High order finite difference and multigrid methods for spatially-evolving instability", *J. Comp. Phys.*, Vol. 106, 1993, pp. 92-100.
25. Johansson, B.C.V., "Boundary conditions for open boundaries for the incompressible Navier-Stokes equation", *J. Comp. Phys.*, Vol. 105, 1993, pp. 233-51.
26. Halpern, L. and Schatzman, M., "Artificial boundary conditions for incompressible viscous flows", *SIAM J. Math. Analysis*, Vol. 20, 1989, pp. 308-353.
27. Sohn, J.L., "Evaluation of FIDAP on some classical laminar and turbulent benchmarks", *Int. J. Numer. Methods Fluids,* Vol. 8, 1988, pp. 1469-90.
28. Durst, F. and Pereira, J.C.F., "Time-dependent laminar backward-facing step flow in a two-dimensional duct", *Journal of Fluids Engineering*, Vol. 110, 1988, pp. 289-96.
29. Armaly, B.F., Durst, F., Pereira, J.C.F. and Schonung, B., "Experimental and theoretical investigation of backward-facing step flow", *J. Fluid Mech.*, Vol. 127, 1983, pp. 473-96.